

Article

miR-130b inhibits proliferation and promotes differentiation in myocytes via targeting Sp1

Yu-Cheng Wang^{1,†}, Xiaohan Yao^{2,†}, Mei Ma², Huihui Zhang², Hui Wang², Lei Zhao³, Shengnan Liu², Chao Sun², Peng Li², Yuting Wu², Xihua Li³, Jingjing Jiang⁴, Yuying Li ², Yan Li^{5,*}, and Hao Ying^{2,6,*}

¹ Shanghai Xuhui District Central Hospital, Zhongshan-Xuhui Hospital, Fudan University, Shanghai 200001, China

² CAS Key laboratory of Nutrition, Metabolism and Food Safety, Shanghai Institute of Nutrition and Health, Chinese Academy of Sciences, Shanghai 200031, China

³ Department of Neuromuscular Disease, Children's Hospital of Fudan University, Shanghai 201102, China

⁴ Department of Endocrinology and Metabolism, Zhongshan Hospital, Fudan University, Shanghai 200031, China

⁵ State Key Laboratory of Food Science and Technology, School of Food Science and Technology, Jiangnan University, Wuxi 214122, China

⁶ Key Laboratory of Food Safety Risk Assessment, Ministry of Health, Beijing 100021, China

[†] These authors contributed equally to this work.

* Correspondence to: Yan Li, E-mail: liyan0520@jiangnan.edu.cn; Hao Ying, E-mail: yinghao@sibs.ac.cn

Edited by Zefeng Wang

Muscle regeneration after damage or during myopathies requires a fine cooperation between myoblast proliferation and myogenic differentiation. A growing body of evidence suggests that microRNAs play critical roles in myocyte proliferation and differentiation transcriptionally. However, the molecular mechanisms underlying the orchestration are not fully understood. Here, we showed that miR-130b is able to repress myoblast proliferation and promote myogenic differentiation via targeting Sp1 transcription factor. Importantly, overexpression of miR-130b is capable of improving the recovery of damaged muscle in a freeze injury model. Moreover, miR-130b expression is declined in the muscle of muscular dystrophy patients. Thus, these results indicated that miR-130b may play a role in skeletal muscle regeneration and myopathy progression. Together, our findings suggest that the miR-130b/Sp1 axis may serve as a potential therapeutic target for the treatment of patients with muscle damage or severe myopathies.

Keywords: miR-130b, muscle regeneration, proliferation, differentiation, Sp1

Introduction

Skeletal muscle is an important organ of the body, which plays a key role in locomotion, exercise, posture maintenance, and energy metabolism (Zhao et al., 2018). Skeletal muscle is mainly composed of satellite cells and multinucleated myofibers (Wei et al., 2018). Myofibers have considerable regenerative capacity after muscle trauma, which guarantees normal function of skeletal muscle (Hu et al., 2018). Skeletal muscle regeneration after muscle injury in adults requires a fine cooperation and balance between myoblast proliferation and myogenic differentiation (Zhu et al., 2018). Even though many key regulators of proliferation and differentiation processes during

skeletal muscle regeneration have been revealed in recent years, a better understanding of the regulation is urgent.

MicroRNAs (miRNAs) are endogenous small non-coding RNAs that regulate target genes expression post-transcriptionally by inhibiting target gene mRNA translation or inducing mRNA degradation (Maan et al., 2018). Recently, miRNAs have been considered as key regulators for myoblast proliferation and myogenic differentiation in skeletal muscle and are thought to be greatly involved in skeletal muscle regeneration as well as myopathies such as muscular dystrophy (O'Leary et al., 2013; Ma et al., 2018). However, whether miRNAs are able to balance myoblast proliferation and differentiation, promote skeletal muscle regeneration, and improve myopathies progression is largely unknown.

miR-130b is located in murine chromosome 16q (homo sapiens chromosome 22q). As described in our previous research, miR-130b is enriched in white adipose tissue and skeletal muscle (Ronkainen et al., 2016), which plays a key role in

Received July 20, 2020. Revised January 8, 2021. Accepted January 8, 2021.

© The Author(s) (2021). Published by Oxford University Press on behalf of *Journal of Molecular Cell Biology*, CEMCS, CAS.

This is an Open Access article distributed under the terms of the Creative Commons Attribution Non-Commercial License (<http://creativecommons.org/licenses/by-nc/4.0/>), which permits non-commercial re-use, distribution, and reproduction in any medium, provided the original work is properly cited. For commercial re-use, please contact journals.permissions@oup.com

metabolic crosstalk between white fat and the muscle (Komiya et al., 2017). In addition, functions of miR-130b have been implicated in mitochondria biogenesis, energy homeostasis, fibrosis, as well as cancer progression (Gomes et al., 2014; Harris et al., 2015; Sargent, 2015; Bosma, 2016). However, the role of miR-130b in myoblast proliferation, differentiation, skeletal muscle regeneration, and pathogenesis of muscular dystrophy remain unknown.

In the present study, we found that miR-130b is able to repress myoblast proliferation and promote myogenic differentiation. Additionally, the regulatory role of miR-130b in myocytes via directly targeting Sp1 was established. Further study showed that miR-130b improves the recovery of damaged muscle, and miR-130b expression in the muscle is decreased in patients with muscular dystrophy. Our findings indicate that miR-130b may

play a pivotal role in skeletal muscle regeneration and myopathy progression. Taken together, our data suggest that miR-130b might serve as a potential therapeutic target for myopathy.

Results

miR-130b represses myoblast proliferation

As myoblast proliferation plays a pivotal role in muscle regeneration, myopathies, as well as muscle dystrophy (Ferraro et al., 2013; Kim et al., 2013; Sakuma et al., 2016), to explore the function of miR-130b in skeletal muscle, we first investigated the effect of miR-130b on C2C12 myoblast proliferation. Interestingly, we found that transfection of miR-130b mimics could inhibit the proliferation of C2C12 myoblasts as evident from a decrease in bromodeoxyuridine (BrdU) incorporation (Figure 1A). Additionally, transfection of specific antisense inhibitor of miR-130b (miR-130b in) was able to

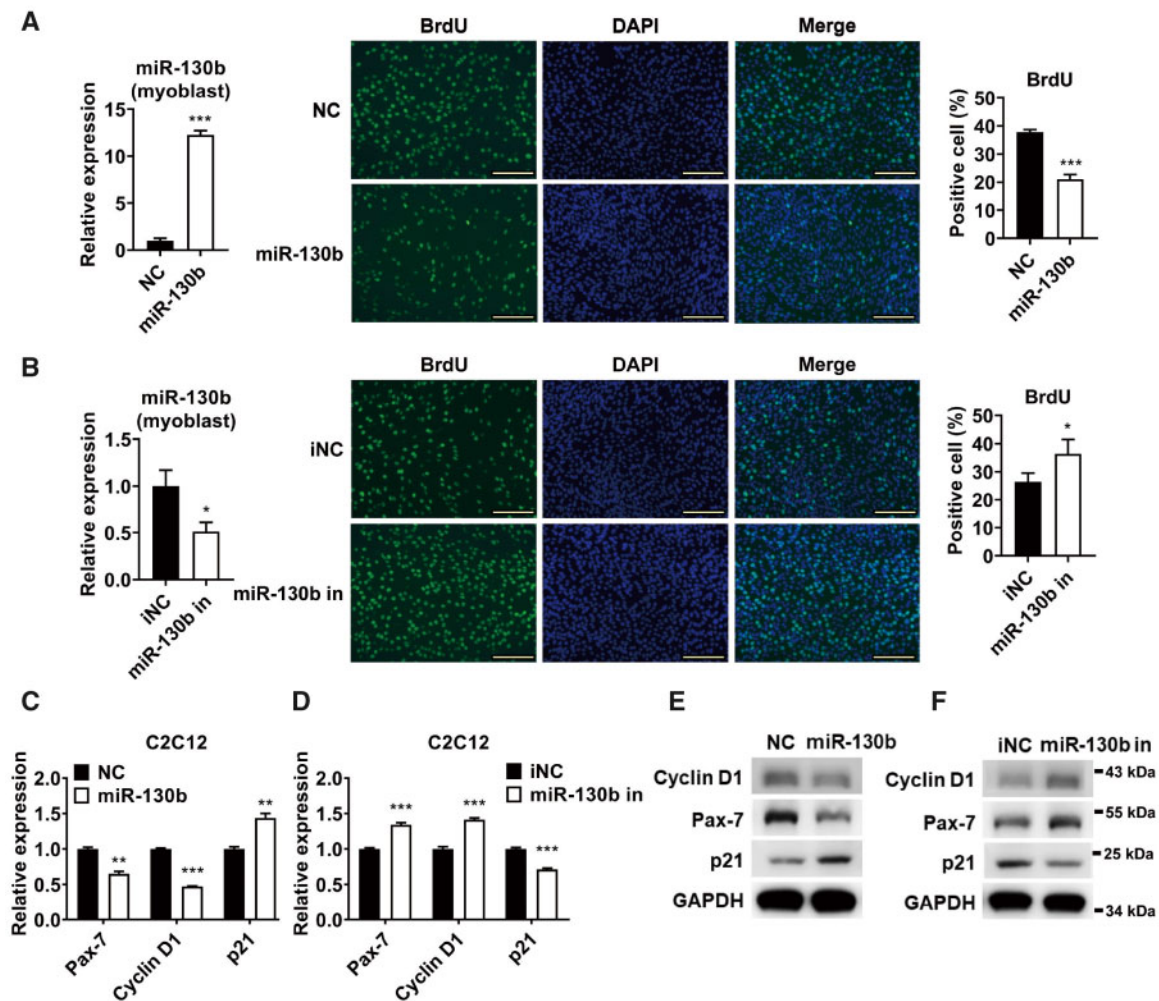


Figure 1 miR-130b inhibits the proliferation in C2C12 myoblasts. Myoblasts were transfected with miR-130b mimics or miR-130b inhibitor. (A and B) The proliferation of C2C12 myoblasts was determined by BrdU incorporation assay. qPCR analysis was performed for miR-130b levels (left). Images of the cells were taken by fluorescence microscope (middle). The percentage of BrdU-positive cells was measured (right, $n = 5$ fields per condition). Scale bar, 200 μm . (C and D) qPCR analysis of the mRNA levels of Pax-7, Cyclin D1, and p21 as indicated. qPCR was performed in triplicate ($n = 3$). (E and F) Western blot analysis of Pax-7, Cyclin D1, and p21 protein levels as indicated. All data are representative of experiments repeated at least twice. * $P < 0.05$, ** $P < 0.01$, *** $P < 0.001$. DAPI, 4',6-diamidino-2-phenylindole; p21, cyclin-dependent kinase inhibitor 1A; GAPDH, glyceraldehyde-3-phosphate dehydrogenase.

promote the growth of C2C12 myoblasts as evident from an increase in BrdU incorporation (Figure 1B). We then analysed the mRNA levels of paired box 7 (Pax-7) and cyclin D1 (two proliferation-associated genes), as well as p21 (an inhibitor of proliferation), in C2C12 myoblasts transfected with miR-130b mimics. Interestingly, the mRNA expression of Pax-7 and Cyclin D1 was decreased, while the mRNA expression of p21 was increased after transfection of miR-130b mimics (Figure 1C). We also checked the effect of miR-130b inhibitor on the mRNA expression of Pax-7, cyclin D1, and p21 in C2C12 myoblasts. As expected, transfection of miR-130b inhibitor led to an increase in Pax-7 and Cyclin D1 mRNA levels and a decrease in p21 mRNA level (Figure 1D). Accordingly, transfection of miR-130b mimics downregulated Pax-7 and cyclin D1 protein levels and elevated p21 protein level, while transfection of miR-130b inhibitor increased Pax-7 and cyclin D1 protein levels and reduced p21 protein level in C2C12 myoblasts (Figure 1E and F). Together, these results indicate that miR-130b acts as a negative regulator of myoblast proliferation.

miR-130b promotes myoblast differentiation

Because p21 is able to trigger cell cycle exit and initiate myoblast terminal differentiation and muscle formation (Zhang et al., 1999), our finding that miR-130b could affect p21 expression (Figure 1C–F) prompted us to investigate the effect of miR-130b on myogenesis. To this end, C2C12 myoblasts were transfected with miR-130b mimics or miR-130b inhibitor followed by induction of myogenic differentiation. We then analysed myotube formation by determining myosin heavy chain (MyHC) expression. Interestingly, we found that transfection of miR-130b mimics could increase myotube formation, while transfection of miR-130b inhibitor led to a significant decrease in myotube formation (Figure 2A and B). Moreover, the mRNA levels of myogenic genes MyoD, MyoG, MYH7, and MEF-2C (Figure 2C and D) and protein levels of MyoG and MEF-2C (Figure 2E) were all elevated by transfection of miR-130b mimics. In agreement, the expression levels of these myogenic genes were all decreased after transfection of miR-130b inhibitor (Figure 2F–H). Together, these data clearly demonstrate that miR-130b is able to promote myoblast differentiation.

Sp1 is a direct target gene of miR-130b

To identify which gene mediates the effect of miR-130b on myoblast proliferation and differentiation, we used TargetScan and miRBase to predict the target gene for miR-130b. Interestingly, we found a putative miR-130b target site in Sp1-3'UTR, which is highly conserved across different species (Figure 3A). Then, we performed western blot and qPCR analyses to examine the expression of Sp1 in C2C12 myoblasts transfected with miR-130b mimics and inhibitors, respectively, for 24 and 48 h (Figure 3B–D). As expected, overexpression of miR-130b decreased both protein and mRNA levels of Sp1 in C2C12 myoblasts (Figure 3B and D, left), while inhibition of miR-130b resulted in an elevation in Sp1 protein (Figure 3C) and mRNA levels (Figure 3D, right). Besides, we found that

overexpression of miR-130b could repress the luciferase activity of a reporter containing Sp1-3'UTR with a miR-130b-responsive element in HEK293T cells. In contrast, inhibition of miR-130b had a promotive effect on the luciferase activity of this reporter (Figure 3E). Although miR-130b and Sp1 have been implicated in skeletal muscle, respectively (Kirkin et al., 2009; Lippai and Low, 2014; Mondal et al., 2019), their expression pattern and relationship have not been well examined. Here, we determined the expression levels of miR-130b and Sp1 at different time points during myoblast differentiation. Intriguingly, the expression level of miR-130b increased gradually during myotube formation, while a significant decline in Sp1 mRNA level was observed upon myogenic differentiation induction (Figure 3F). Moreover, the mRNA levels of miR-130b and Sp1 in different types of skeletal muscle were determined. We observed the highest level of miR-130b whereas the lowest level of Sp1 in fast-twitch tibial anterior (TA) muscles (Figure 3G and H). Together, these results suggest that Sp1 is a direct target gene of miR-130b in muscle cells.

miR-130b modulates myoblast proliferation and differentiation through Sp1

To examine the role of Sp1 in C2C12 myoblast proliferation and differentiation, BrdU incorporation assay and MyHC or MF20 immunostaining were performed. As expected, overexpression of Sp1 by transfection of Sp1 expression plasmids could promote C2C12 myoblast proliferation as evident from an increase in BrdU incorporation (Figure 4A). Moreover, overexpression of Sp1 could decrease C2C12 myotube formation (Figure 4B). Accordingly, inhibition of Sp1 by using specific small interfering RNA (siRNA, si-Sp1) could increase myotube formation in mouse satellite cells (Figure 4C and D). Consistently, Sp1 overexpression could elevate both mRNA and protein levels of Pax-7 and cyclin D1 (Figure 4E and G), while Sp1 inhibition could decrease Pax-7 and cyclin D1 levels (Figure 4F and H) in C2C12 myoblasts. Furthermore, overexpression of Sp1 could repress the mRNA and protein levels of myogenic genes and p21 (Figure 4I and K), while downregulation of Sp1 could increase these levels (Figure 4J and L) in C2C12 myotubes. Importantly, both the inhibitory effect of miR-130b on myoblast proliferation and the promotion of myotube formation were attenuated by Sp1 overexpression (Figure 4M–R), suggesting that Sp1 might mediate the effects of miR-130b during myogenesis.

miR-130b is implicated in skeletal muscle regeneration and dystrophy

To investigate the role of miR-130b in skeletal muscle regeneration *in vivo*, a freeze injury model was used as described previously (O'Leary et al., 2013). We first determined the mRNA levels of miR-130b and Sp1 in gastrocnemius (GAS) muscles at the indicated time points following freeze injury, and found that the miR-130b expression level decreased 7 days after

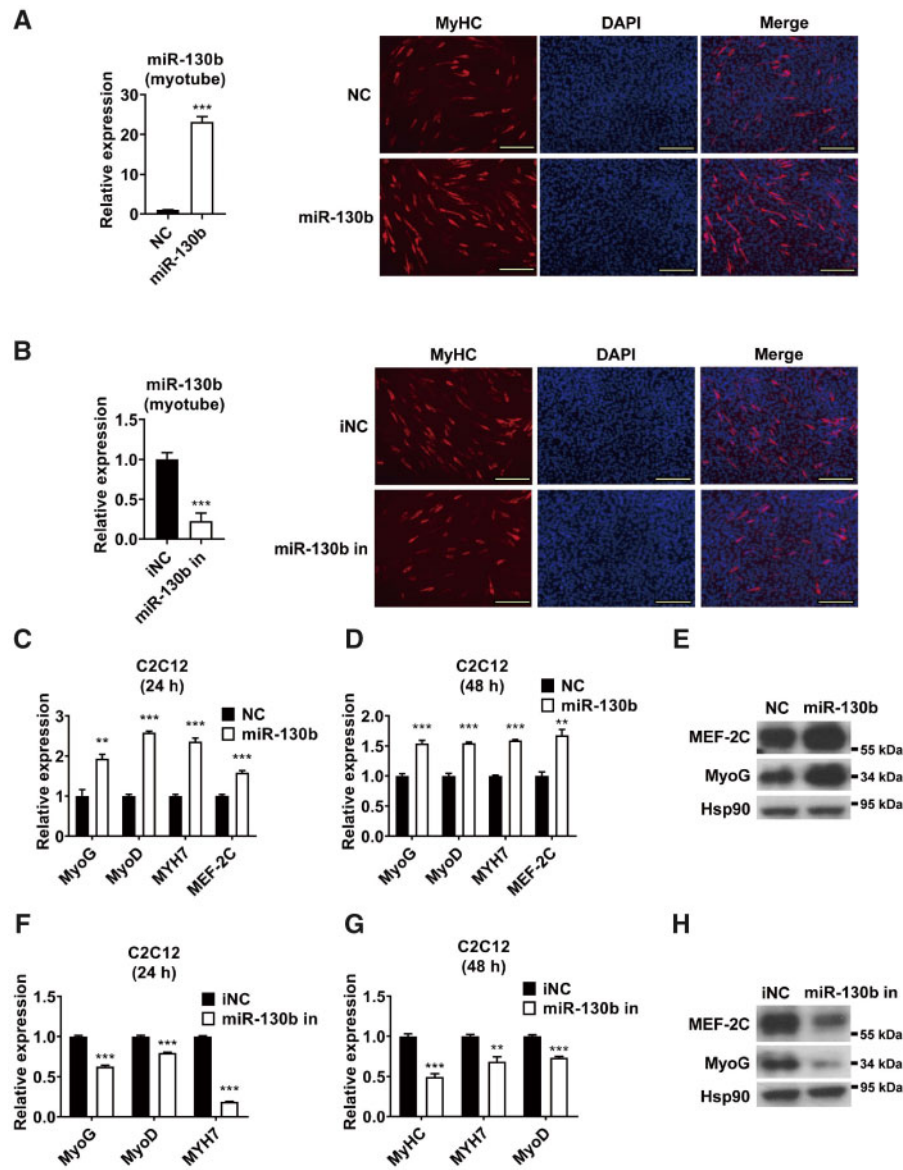


Figure 2 miR-130b promotes myoblast differentiation. C2C12 myoblasts were transfected with miR-130b mimics or miR-130b inhibitor as indicated, followed by induction of myogenic differentiation, and then harvested after 24 (C and F) or 48 h (A, B, D, E, G, H). (A and B) qPCR analysis of miR-130b levels in C2C12 myotubes transfected with miR-130b mimics or miR-130b inhibitor (left). Immunostaining of C2C12 myotubes was performed by using an antibody against MyHC (right, $n = 5$ fields per condition). Scale bar, 200 μ m. (C, D, F, G) qPCR analysis of the mRNA levels of MyoG, MyoD, MYH7, and MEF-2C in C2C12 cells. qPCR was performed in triplicate ($n = 3$). (E and H) Western blot analysis of MyoG and MEF-2C protein levels in C2C12 cells. All data are representative of experiments repeated at least twice. $**P < 0.01$, $***P < 0.001$. MyoG, myogenin; MyoD, myogenic differentiation; MEF-2C: myocyte enhancer factor 2C; MYH7: myosin heavy chain 7; Hsp90: heat shock protein 90.

injury and then elevated gradually (Figure 5A). On the contrary, the Sp1 mRNA level reached the peak at Day 7 after freeze injury (Figure 5B). To test whether manipulation of miR-130b expression could affect muscle regeneration *in vivo*, miR-130b mimics or miR-130b inhibitor was electro-transferred into the freeze-injured GAS muscles of mice. As expected, overexpression of miR-130b decreased Sp1 mRNA level in GAS muscles, while electro-transfection of miR-130b inhibitor resulted in an elevation in Sp1 mRNA level (Figure 5C and D). Interestingly, miR-130b

overexpression led to increased mRNA levels of myogenic genes in GAS muscles 7 days after injury (Figure 5E), while downregulation of miR-130b resulted in a decrease in the mRNA levels of these myogenic genes (Figure 5F). Consistently, MyHC protein level was elevated significantly in GAS muscles of mice with miR-130b overexpression (Figure 5G), while it was decreased in mice with miR-130b downregulation (Figure 5H). Moreover, muscle regeneration was greatly enhanced in GAS muscles with miR-130b overexpressing as shown by hematoxylin and eosin (H&E) staining at Days 7,

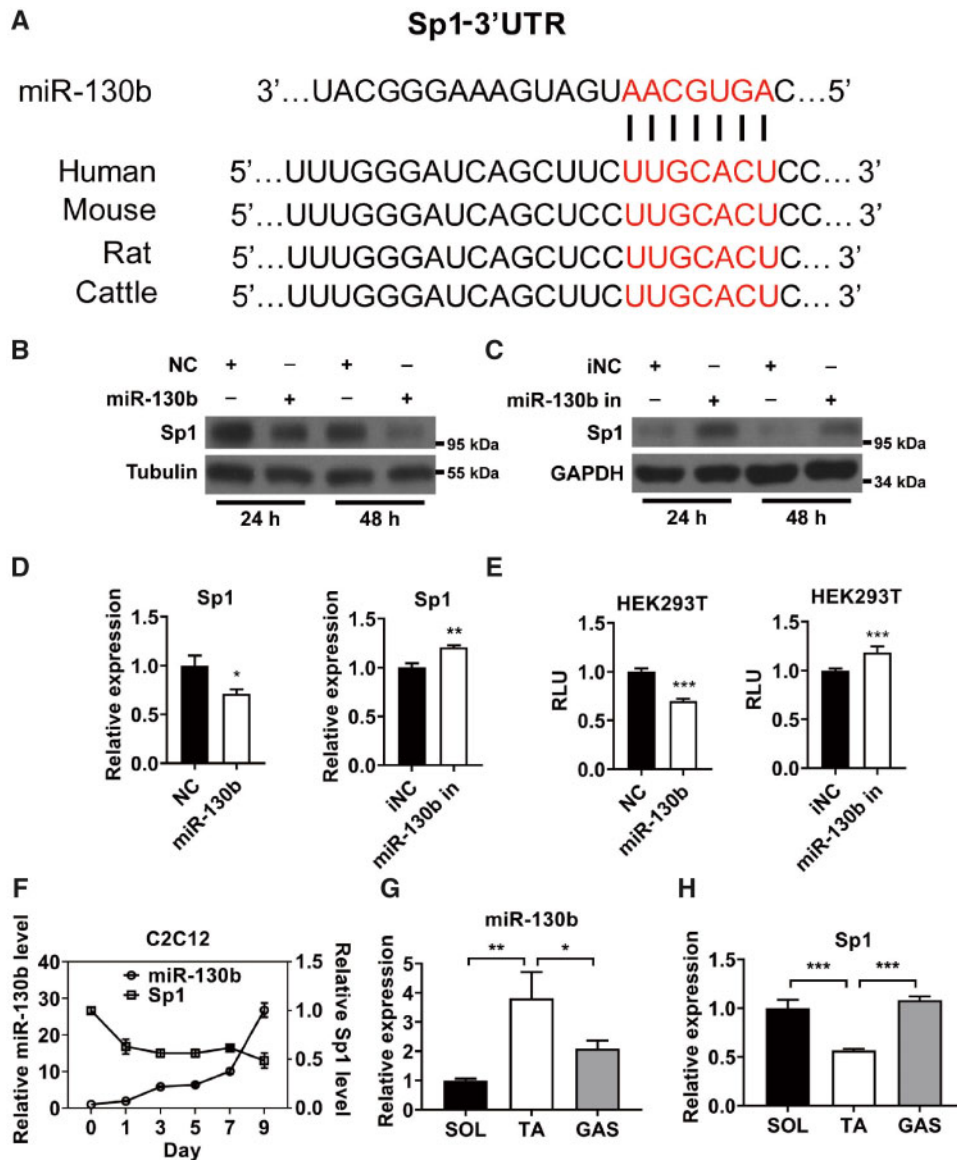


Figure 3 Sp1 is a direct target gene of miR-130b. **(A)** Sequence alignment of Sp1-3'UTR and miR-130b reveals a miR-130b-responsive element. The seed sequence is highlighted in red. Conserved miR-130b-responsive elements in the Sp1-3'UTR fragments from different species are shown. **(B and C)** Western blot analysis of Sp1 protein levels in C2C12 myoblasts as indicated for 24 and 48 h. **(D)** qPCR analysis of the mRNA levels of Sp1 in C2C12 myoblasts as indicated. qPCR was performed in triplicate ($n = 3$). **(E)** Luciferase assay for the activity of the reporter containing Sp1-3'UTR with a putative miR-130b-responsive element in HEK293T cells transfected with miR-130 mimics (left) or miR-130b inhibitor (right). The assay was performed in triplicate ($n = 3$). **(F)** qPCR analysis of miR-130b and Sp1 time-course expression upon the induction of C2C12 myoblast differentiation. qPCR was performed in triplicate ($n = 3$). **(G and H)** qPCR analysis of the mRNA levels of miR-130b **(G)** and Sp1 **(H)** in the soleus (SOL), TA, and GAS muscles of mice ($n = 3$ mice per group). All data are representative of experiments repeated at least twice. * $P < 0.05$, ** $P < 0.01$, *** $P < 0.001$.

14, and 21 after freeze injury (Figure 5). Importantly, an increased number of regenerated myofibers (eMyHC-positive) whereas a decreased number of Pax-7-positive cells were observed in GAS muscles with miR-130b overexpression at Day 7 after injury (Figure 5) and K). Collectively, these findings suggest that miR-130b plays a regulatory role in muscle regeneration.

Lastly, we examined the expression levels of miR-130b and Sp1 in Dmd mutant (mdx) mice and patients with Duchenne

muscular dystrophy (DMD) or less severe Becker muscular dystrophy (BMD). As expected, miR-130b expression was decreased in GAS muscles of mdx mice (Figure 6A), which was accompanied by an elevation in both mRNA and protein levels of Sp1 (Figure 6B and C). We also found that miR-130b expression was decreased in BMD patients and further decreased in DMD patients, suggesting that miR-130b level might be negatively correlated with the severity of myopathy (Figure 6D).

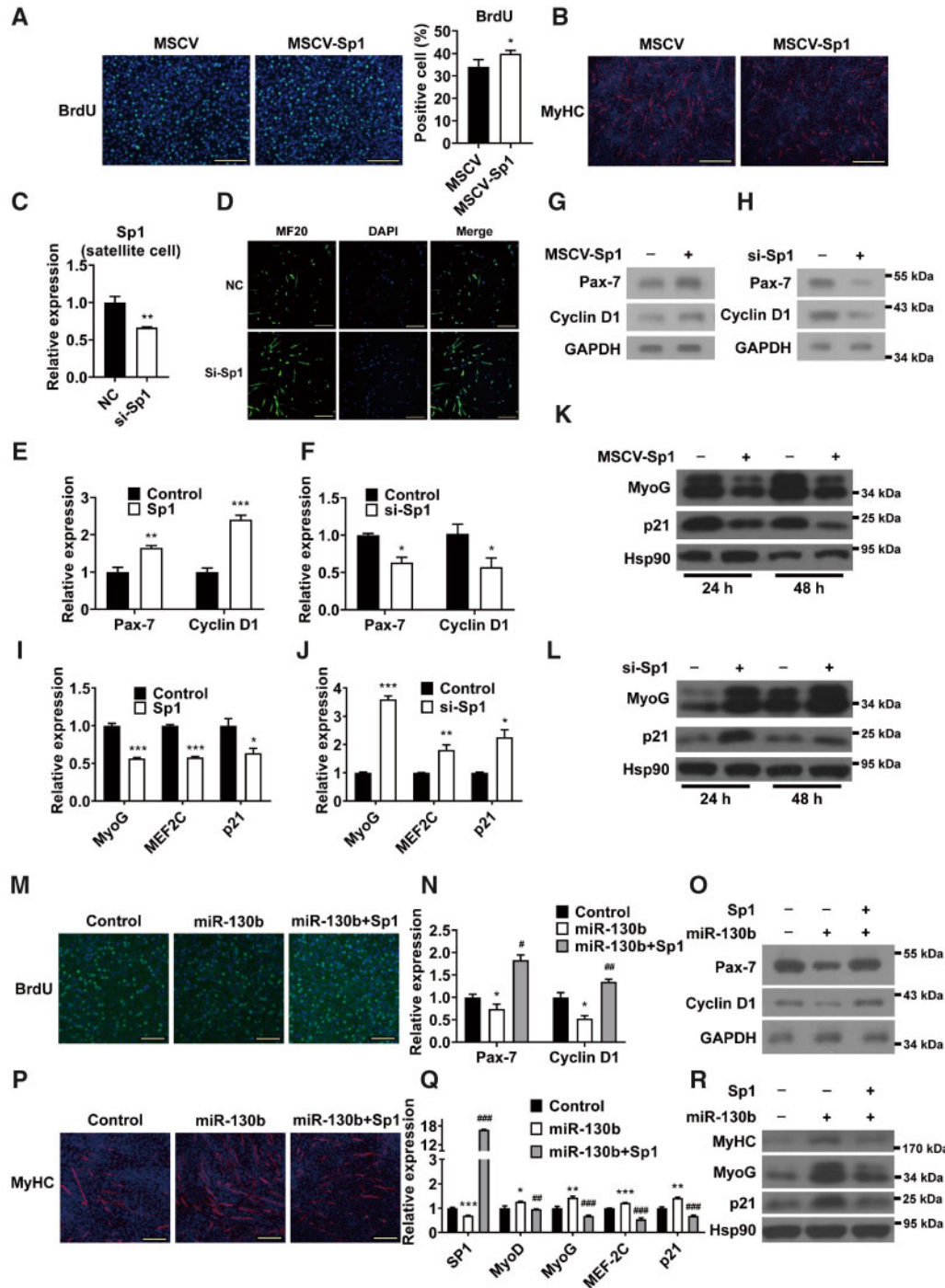


Figure 4 miR-130b modulates myoblast proliferation and differentiation through Sp1. (A and B) C2C12 myoblasts were transfected with Sp1 expression plasmids (MSCV-Sp1) or control vectors (MSCV) followed by induction of myogenic differentiation. (A) The proliferation of C2C12 myoblasts was examined by BrdU incorporation assay. Images of the cells were taken by fluorescence microscope (left). The percentage of BrdU-positive cells was measured (right, $n = 5$ fields per condition). (B) Immunostaining of C2C12 myotubes was performed by using an antibody against MyHC. (C and D) Mouse muscle satellite cells were transfected with control or si-Sp1 oligos, followed by induction of myogenic differentiation for 2 days. qPCR analysis was performed for Sp1 mRNA levels (C) and photographs of MF20 immunofluorescence staining were taken (D). (E–H) C2C12 myoblasts were transfected with Sp1 expression plasmids (MSCV-Sp1 or MSCV) or si-Sp1 oligos (E–H), followed by induction of myogenic differentiation (I–L) as indicated. (E–H) qPCR and western blot analyses of Pax-7 and cyclin D1 expression levels as indicated. (I–L) qPCR and western blot analyses of MyoG, MEF-2C, and p21 expression levels as indicated. (M–R) C2C12 myoblasts were transfected with miR-130b mimics with or without Sp1 expression plasmids (MSCV-Sp1) (M–O), followed by induction of myogenic differentiation (P–R) as indicated. BrdU incorporation assay (M), qPCR analysis (N and Q), western blot analysis (O and R), and immunostaining of C2C12 myotubes (P) were performed as indicated. All cells were harvested for analysis 2 days post-transfection unless otherwise indicated (K and L). Scale bar, 200 μm (A, B, D, M, and P). All data are representative of experiments repeated at least twice. qPCR was performed in triplicate ($n = 3$). * $P < 0.05$, ** $P < 0.01$, *** $P < 0.001$.

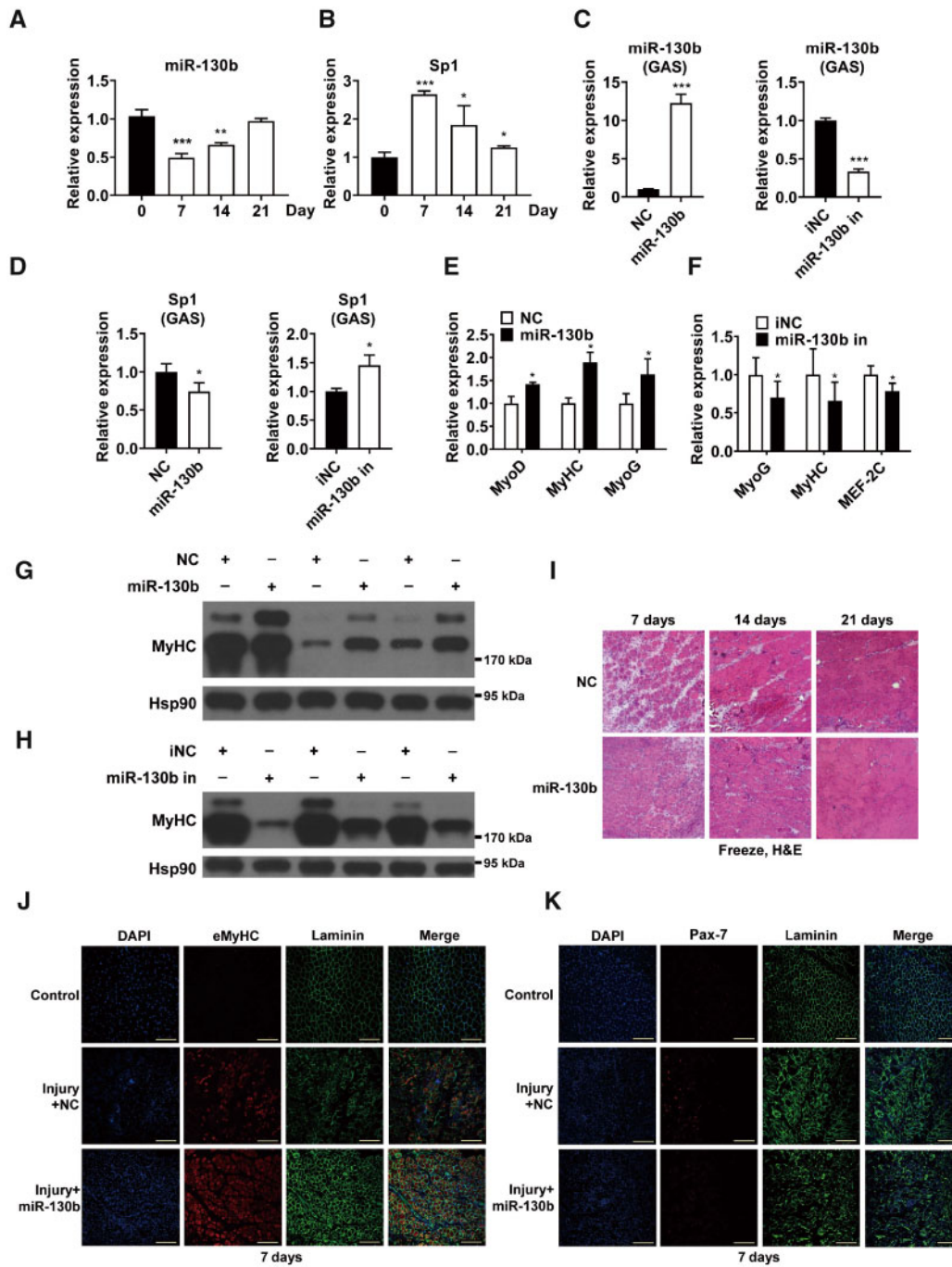


Figure 5 miR-130b facilitates muscle regeneration after injury. (A and B) qPCR analysis of miR-130b (A) and Sp1 (B) time-course expression in GAS muscles of mice following freeze injury. (C–H) qPCR analysis of the mRNA levels of miR-130b (C), Sp1 (D), and myogenic genes (E and F) and western blot analysis of MyHC protein levels (G and H) in GAS muscles of mice 7 days after free injury followed with electro-transfer of miR-130b mimics or miR-130b inhibitor as indicated. (I) H&E staining of GAS muscles of mice at the indicated time points after freeze injury followed with or without electro-transfer of miR-130b mimics. (J and K) Immunofluorescence staining of eMyHC, Pax-7, and Laminin in GAS muscles of mice treated as indicated 7 days after freeze injury. Scale bar, 200 μ m. All data are representative of experiments repeated at least twice. qPCR was performed in triplicate ($n = 3$). * $P < 0.05$, ** $P < 0.01$, *** $P < 0.001$.

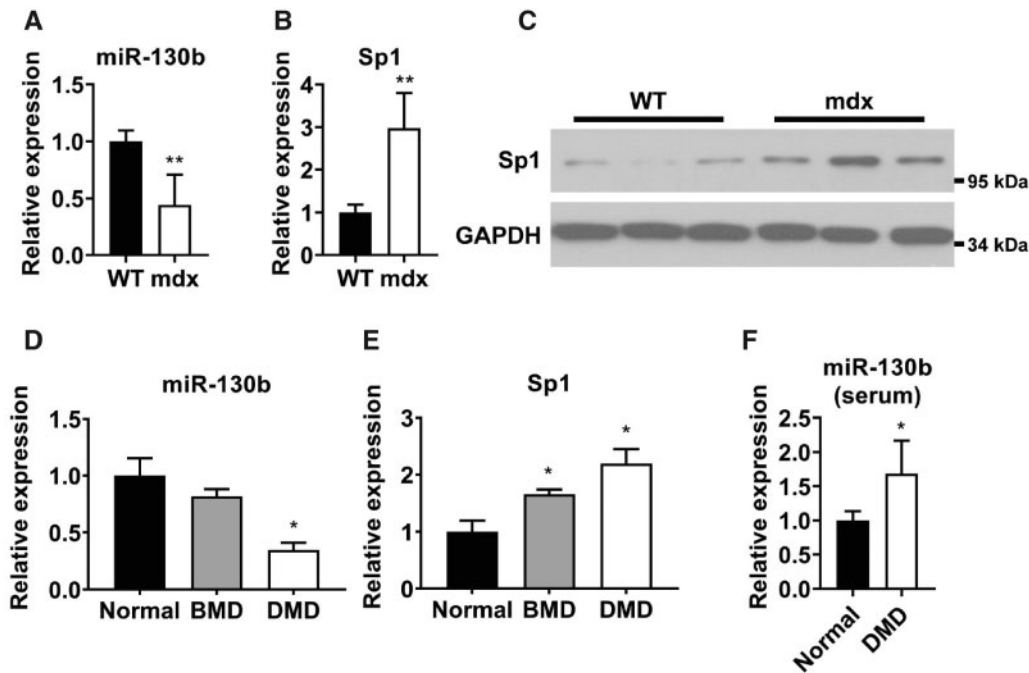


Figure 6 miR-130b is implicated in the pathogenesis of muscular dystrophy. (A and B) qPCR analysis of the mRNA levels of miR-130b (A) and Sp1 (B) in GAS muscles of WT and mdx mice ($n = 5$ mice per group). (C) Western blot analysis of Sp1 protein levels in GAS muscles of WT and mdx mice ($n = 3$ mice per group). (D and E) qPCR analysis of the mRNA levels of miR-130b (D) and Sp1 (E) in the muscle biopsy samples obtained from normal subjects (Normal) and patients with DMD or less severe BMD ($n = 5-17$). (F) qPCR analysis of the circulating levels of miR-130b in serum samples from normal subjects and patients with DMD ($n = 5$ per group). qPCR was performed in triplicate. $*P < 0.05$, $**P < 0.01$.

Accordingly, the mRNA levels of Sp1 were significantly increased in BMD and DMD patients (Figure 6E). Since circulating miRNAs could serve as promising biomarkers for DMD diagnosis, we also measured miR-130b level in the serum and found that the level of circulating miR-130b was higher in DMD patients than that in normal subjects (Figure 6F).

Taken together, our *in vivo* data indicated that miR-130b acts as a positive regulator of skeletal muscle regeneration and the downregulation of miR-130b might be involved in the pathogenesis of muscular dystrophy.

Discussion

Understanding the molecular mechanisms underlying muscle regeneration will help us to improve the management of muscle damage or severe myopathies. When muscle damage or myopathy occurs, the satellite cells are activated and become myoblasts, then proliferate and differentiate into myotubes, and then form myofibers (He et al., 2004). Most muscle disorders are accompanied by abnormal myoblast proliferation and myogenic differentiation (Nunez et al., 1975). In addition, growing evidence has indicated that miRNA functions as a key regulator during myoblast proliferation and myogenic differentiation (Altshuler-Keylin et al., 2016; Lu et al., 2018). Here, we attempt to focus our study on the function of miR-130b in skeletal muscle. Our results demonstrated that the levels of miR-130b were gradually elevated in myocytes during differentiation, while

they were decreased and gradually restored to nearly normal level in injured muscle, suggesting that miR-130b may be involved in the regeneration of the muscle.

It has been reported that miR-130b plays a key role in mitochondria biogenesis, energy homeostasis, fibrosis, and cancer progression (Gomes et al., 2014; Harris et al., 2015; Sargent, 2015; Bosma, 2016); however, its function in skeletal muscle is largely unknown. In this study, the effects of miR-130b overexpression and inhibition were investigated by transfection with miR-130b mimics and miR-130b inhibitor, respectively. Our data indicated that miR-130b could repress myoblast proliferation, an early stage of skeletal muscle regeneration. In addition, when miR-130b was overexpressed, myotube formation and myogenic markers were significantly increased in C2C12 myocytes, suggesting that miR-130b could promote myogenic differentiation. To be noted, miR-130b level declined in damaged muscle 7 days after freeze injury, which might facilitate the proliferation of muscle progenitor cells in the early stage of muscle regeneration. However, the upstream stimuli that control miR-130b expression during muscle regeneration remain unknown and require further study.

Our results also unravel a novel function of miR-130b in regulating proliferation and differentiation of myoblasts via direct targeting Sp1, a vital transcriptional factor. Although the effect of Sp1 knockdown on the proliferation and differentiation of bovine skeletal muscle satellite cells have been examined

(Lippai and Low, 2014), the role of Sp1 in mouse myoblast proliferation and differentiation was largely unknown. In this study, we confirmed the pro-proliferative role of Sp1 in C2C12 myoblasts (Figure 4A). In contrast to the previous report, we found that Sp1 overexpression could inhibit C2C12 myoblast differentiation, as evident from a decrease in MyoG and p21, while Sp1 suppression was able to promote C2C12 myoblast differentiation, as evident from increased expression of MyoG and p21 (Figure 4C and D). Importantly, we found that overexpression of Sp1 could attenuate the effect of miR-130b overexpression on the myogenic markers (MyoG, MyoD, and MEF-2C) and the regulator of both myoblast proliferation and differentiation (p21) in C2C12 myocytes (Zhang et al., 1999). Based on these data, we speculated that Sp1 might mediate the action of miR-130b during myogenesis (Figure 4).

It has been suggested that the repression of myogenic differentiation not only decelerates muscle regeneration after injury but also contributes to the pathogenesis of many myopathies, such as DMD (Bosma et al., 2012; Broskey et al., 2013). In line with our current knowledge, the expression level of miR-130b was attenuated in GAS muscles of mdx mice, while Sp1 expression was elevated (Figure 6A and B). Consistently, miR-130b level markedly declined whereas Sp1 level dramatically increased in DMD patients compared to normal subjects. Moreover, miR-130b overexpression *in vivo* could accelerate the muscle repair after freeze injury, suggesting that miR-130b might play a role in muscle regeneration. Thus, our finding also offers a novel strategy to treat muscle pathologies.

Taken together, the regulatory role of miR-130b/Sp1 axis in myocytes discovered in this study is important to improve our understanding of skeletal muscle regeneration. As the levels of miR-130b are downregulated in the specimens from DMD patients, overexpression of miR-130b might serve as a potential therapeutic strategy to treat patients with muscle damage or severe myopathies.

Materials and methods

In vivo study

In this study, 8–12 weeks old male mice were used. All experimental procedures and protocols were reviewed and approved by the Institutional Review Board of Shanghai Institute of Nutrition and Health, Chinese Academy of Sciences. C57BL/6J wild-type (WT), and mdx mice were obtained from Model Animal Research Center of Nanjing University and maintained as described previously (Rossetti et al., 2018). Freeze injury model was induced by a single freeze injury of GAS muscles as described before with modification (Fan et al., 2017). Briefly, under anesthesia, the skin of GAS muscles was shaved and exposed. Injury was induced by applying a steel bar cooled in liquid nitrogen to the GAS muscles for 20 sec (Mann et al., 2016). After 24 h, mice were subjected to electroporation. *In vivo* muscle transfection by electroporation was performed according to the protocol described before with modification (Zhang et al., 2014). Briefly, oligo pellets of miR-130b mimics or inhibitor

were resuspended in phosphate-buffered saline (PBS) and injected into GAS muscles by using a syringe (20 μ mol/50 μ l PBS). Then, five electric pulses (20 ms duration at an interval of 200 ms, voltage to distance ratio 50 V/cm) were given by using an electric pulse generator (BTX; ECM-830). After 7, 14, or 21 days of injury, mice were anesthetized. GAS muscles were dissected and frozen in liquid nitrogen. The human skeletal muscle specimens from patients with BMD or DMD were obtained during surgery after obtaining their written informed consent at Children's Hospital of Fudan University. All the procedures were reviewed and approved by the Ethics Committee of Fudan University and informed consent was obtained from all patients. Tissues or human muscle specimens were harvested and frozen in liquid nitrogen and store at -80°C until further analysis.

Cell culture, transfection, and luciferase assay

Mouse C2C12 myoblast cells and human HEK293T cells were cultured in Dulbecco's modified Eagle medium supplemented with 10% fetal bovine serum (Gibco), 100 units/ml penicillin, and 100 mg/ml streptomycin. To induce myogenic differentiation, fetal bovine serum was replaced by horse serum (2%, final concentration, Gibco) in culture medium. Mouse satellite cells were isolated and cultured as described before (Li et al., 2020). Cells were maintained in a humidified incubator at 37°C and 5% CO_2 atmosphere. Plasmids and RNA oligonucleotides were transfected into myoblasts or satellite cells by using Lipofectamine 2000 and Lipofectamine 3000 (Invitrogen). To analyse the effect of miR-130b or Sp1 on myogenesis, after transfection, cells were subject to myogenic differentiation, and then harvested for further analysis 2 days post-transfection unless otherwise indicated. Luciferase assay was performed by using Dual-Luciferase Reporter Assay System (Promega) following the manufacturer's instructions and luminometer (Berthold Technologies).

Plasmids and RNA oligonucleotides

For construction of expression plasmid and luciferase reporter plasmids, the coding sequence region and the Sp1-3'UTR fragment were amplified from mouse cDNA and inserted into CMV and pRL-TK vectors. GMR-miRTM miRNA double-stranded mimics for miR-130b (CAGUGCAAUGAUGAAAGGGCAU) and inhibitor for miR-130b (AUGCCCUUCAUCAUJGCACUG) were obtained from GenePharma. Nonsense sequences were used as negative control (UCACAACCUCCUAGAAAGAGUAGA) and inhibitor control (UCUACUCUUUCUAGGAGGUUGUGA).

Western blot and qPCR analyses

Radio-immunoprecipitation assay (RIPA) lysis buffer (50 mM Tris-HCl, pH 7.5, 150 mM NaCl, 1.0 mM EDTA, 0.1% sodium dodecyl sulfate, 1% sodium deoxycholate, and 1% Triton X-100) was used to prepare cell or frozen tissue protein lysates. The protein concentration was determined by using BCA protein assay kit (Thermo) following the instructions. Protein lysates

were resolved on 10% SDS-PAGE gels using standard procedures. Anti-Sp1 (106 kDa; Santa Cruz), anti-Pax7 (44–50 kDa; Santa Cruz), anti-Cyclin D1 (37 kDa; Santa Cruz), anti-MEF-2C (40–65 kDa; Santa Cruz), anti-MyoG (34 kDa; Santa Cruz), anti-MyHC (200 kDa; Santa Cruz), anti-p21 (21 kDa; Santa Cruz), anti-Tubulin (55 kDa; Sigma Aldrich), anti-GAPDH (36 kDa; Sigma Aldrich), and anti-HSP90 (90 kDa; Cell Signaling Technology) were used for western blot analysis.

Trizol reagent (Thermo) was used to extract total RNA from cells or frozen tissues according to the standard procedure. First strand cDNA was synthesized by using the PrimeScript RT kit (TaKaRa). The miRNAs were reverse transcribed by stem-loop RT system, which was performed as described previously (Liu et al., 2014). qPCR was performed on an ABI7900 Real Time PCR System (Applied Biosystems). The detailed information of PCR primers is in [Supplementary Table S1](#).

Immunostaining

Immunostaining of BrdU-positive myoblasts, MyHC, and MF20 in myotubes was performed as described previously (O'Leary et al., 2013; Hwang et al., 2014; Zhang et al., 2014). For BrdU incorporation assay, after transfection, myoblasts were incubated with 10 µg/ml BrdU (Sigma-Aldrich) for 2 h before harvest. For MyHC and MF20 staining, after transfection, myoblasts were subjected to myogenic differentiation for 2 days. Cells were fixed with cold methanol, and then blocked with 3% bovine serum albumin in PBS for 1 h, followed by incubation with primary antibodies for BrdU (Santa Cruz), MyHC (Santa Cruz), and MF20 (DSHB) for 2 h. Alexa Fluor 488 anti-mouse IgG1 (Invitrogen) or Alexa Fluor 594 anti-rabbit IgG1 (Invitrogen) was added as secondary antibodies for 1 h at room temperature.

Statistical analysis

All data are representative of experiments repeated at least twice or three times. qPCR analysis and luciferase assay were performed in triplicate. GraphPad Prism 8.0 was applied to all statistical analyses. Data are presented as mean ± SD. Student's *t*-test was performed to assess whether the means of two groups are statistically significant from each other ($P < 0.05$).

Supplementary material

[Supplementary material](#) is available at *Journal of Molecular Cell Biology* online.

Funding

This work was supported by grants from the National Natural Science Foundation of China (81570768 to Y.-C.W., 31900841 to Yan Li, 91957205 and 31525012 to H.Y., and 81471016 to J.J.), the Ministry of Science and Technology of China (2016YFA0500102 and 2016YFC1304905), CAS Key Laboratory of Nutrition,

Metabolism and Food Safety (KLNMF2019-01), and Chinese Academy of Sciences Interdisciplinary Innovation Team.

Conflict of interest: none declared.

Author contributions: Y.-C.W., Yan Li, and H.Y. conceived and designed the study; Y.-C.W., X.Y., M.M., H.Z., Yuying Li, and Yan Li carried out the study; H.W., Yuying Li, L.Z., S.L., C.S., P.L., Y.W., X.L., and J.J. contributed new reagents/analytic tools; X.Y., Yan Li, and H.Y. analysed data; Y.-C.W., Yuying Li, and J.J. contributed to discussion and supervised the project; and Yan Li and H.Y. wrote the paper.

References

- Altshuler-Keylin, S., Shinoda, K., Hasegawa, Y., et al. (2016). Beige adipocyte maintenance is regulated by autophagy-induced mitochondrial clearance. *Cell Metab.* *24*, 402–419.
- Bosma, M. (2016). Lipid droplet dynamics in skeletal muscle. *Exp. Cell Res.* *340*, 180–186.
- Bosma, M., Minnaard, R., Sparks, L.M., et al. (2012). The lipid droplet coat protein perilipin 5 also localizes to muscle mitochondria. *Histochem. Cell Biol.* *137*, 205–216.
- Broskey, N.T., Daraspe, J., Humbel, B.M., et al. (2013). Skeletal muscle mitochondrial and lipid droplet content assessed with standardized grid sizes for stereology. *J. Appl. Physiol.* *115*, 765–770.
- Fan, J., Yang, X., Li, J., et al. (2017). Spermidine coupled with exercise rescues skeletal muscle atrophy from D-gal-induced aging rats through enhanced autophagy and reduced apoptosis via AMPK–FOXO3a signal pathway. *Oncotarget* *8*, 17475–17490.
- Ferraro, E., Giammarioli, A.M., Caldarola, S., et al. (2013). The metabolic modulator trimetazidine triggers autophagy and counteracts stress-induced atrophy in skeletal muscle myotubes. *FEBS J.* *280*, 5094–5108.
- Gomes, A.F., Magalhaes, K.G., Rodrigues, R.M., et al. (2014). Toxoplasma gondii-skeletal muscle cells interaction increases lipid droplet biogenesis and positively modulates the production of IL-12, IFN-γ and PGE₂. *Parasit. Vectors* *7*, 47.
- Harris, L.A., Skinner, J.R., Shew, T.M., et al. (2015). Perilipin 5-driven lipid droplet accumulation in skeletal muscle stimulates the expression of fibroblast growth factor 21. *Diabetes* *64*, 2757–2768.
- He, J., Goodpaster, B.H., and Kelley, D.E. (2004). Effects of weight loss and physical activity on muscle lipid content and droplet size. *Obes. Res.* *12*, 761–769.
- Hu, Y., Sun, Q., Hu, Y., et al. (2018). Corticosterone-induced lipogenesis activation and lipophagy inhibition in chicken liver are alleviated by maternal betaine supplementation. *J. Nutr.* *148*, 316–325.
- Hwang, Y., Suk, S., Shih, Y.R., et al. (2014). WNT3A promotes myogenesis of human embryonic stem cells and enhances in vivo engraftment. *Sci. Rep.* *4*, 5916.
- Kim, Y.A., Kim, Y.S., Oh, S.L., et al. (2013). Autophagic response to exercise training in skeletal muscle with age. *J. Physiol. Biochem.* *69*, 697–705.
- Kirkin, V., McEwan, D.G., Novak, I., et al. (2009). A role for ubiquitin in selective autophagy. *Mol. Cell* *34*, 259–269.
- Komiya, Y., Sawano, S., Mashima, D., et al. (2017). Mouse soleus (slow) muscle shows greater intramyocellular lipid droplet accumulation than EDL (fast) muscle: fiber type-specific analysis. *J. Muscle Res. Cell Motil.* *38*, 163–173.
- Li, Y., Yuan, J., Chen, F., et al. (2020). Long noncoding RNA SAM promotes myoblast proliferation through stabilizing Sugt1 and facilitating kinetochore assembly. *Nat. Commun.* *11*, 2725.

- Lippai, M., and Low, P. (2014). The role of the selective adaptor p62 and ubiquitin-like proteins in autophagy. *BioMed Res. Int.* 2014, 832704.
- Liu, W., Cao, H., Ye, C., et al. (2014). Hepatic miR-378 targets p110 α and controls glucose and lipid homeostasis by modulating hepatic insulin signaling. *Nat. Commun.* 5, 5684.
- Lu, X., Altshuler-Keylin, S., Wang, Q., et al. (2018). Mitophagy controls beige adipocyte maintenance through a Parkin-dependent and UCP1-independent mechanism. *Sci. Signal.* 11, eaap8526.
- Ma, Y., Zhou, Y., Zhu, Y.C., et al. (2018). Lipophagy contributes to testosterone biosynthesis in male rat leydig cells. *Endocrinology* 159, 1119–1129.
- Maan, M., Peters, J.M., Dutta, M., et al. (2018). Lipid metabolism and lipophagy in cancer. *Biochem. Biophys. Res. Commun.* 504, 582–589.
- Mann, S., Abuelo, A., Nydam, D.V., et al. (2016). Insulin signaling and skeletal muscle atrophy and autophagy in transition dairy cows either overfed energy or fed a controlled energy diet prepartum. *J. Comp. Physiol. B* 186, 513–525.
- Mondal, S., Roy, D., Sarkar Bhattacharya, S., et al. (2019). Therapeutic targeting of PFKFB3 with a novel glycolytic inhibitor PFK158 promotes lipophagy and chemosensitivity in gynecologic cancers. *Int. J. Cancer* 144, 178–189.
- Nunez, E.A., Hagopian, M., and Gershon, M.D. (1975). Lipid droplet accumulation in cardiac muscle cells of the bat: potential auto-toxicity of the cardiac sympathetic innervation. *Anat. Rec.* 181, 149–169.
- O'Leary, M.F., Vainshtein, A., Iqbal, S., et al. (2013). Adaptive plasticity of autophagic proteins to denervation in aging skeletal muscle. *Am. J. Physiol. Cell Physiol.* 304, 422–430.
- Ronkainen, J., Mondini, E., Cinti, F., et al. (2016). Fto-deficiency affects the gene and microRNA expression involved in brown adipogenesis and browning of white adipose tissue in mice. *Int. J. Mol. Sci.* 17, 1851.
- Rossetti, M.L., Steiner, J.L., and Gordon, B.S. (2018). Increased mitochondrial turnover in the skeletal muscle of fasted, castrated mice is related to the magnitude of autophagy activation and muscle atrophy. *Mol. Cell. Endocrinol.* 473, 178–185.
- Sakuma, K., Kinoshita, M., Ito, Y., et al. (2016). p62/SQSTM1 but not LC3 is accumulated in sarcopenic muscle of mice. *J. Cachexia Sarcopenia Muscle* 7, 204–212.
- Sargent, J. (2015). Metabolism: the lipid-droplet-coating protein perilipin-5 in fast-twitch muscle fibres confers metabolic protection. *Nat. Rev. Endocrinol.* 11, 316.
- Wei, C.C., Luo, Z., Hogstrand, C., et al. (2018). Zinc reduces hepatic lipid deposition and activates lipophagy via Zn²⁺/MTF-1/PPAR α and Ca²⁺/CaMKK β /AMPK pathways. *FASEB J.* 32, 6666–6680.
- Zhang, D., Wang, X., Li, Y., et al. (2014). Thyroid hormone regulates muscle fiber type conversion via miR-133a1. *J. Cell Biol.* 207, 753–766.
- Zhang, P., Wong, C., Liu, D., et al. (1999). p21^{CIP1} and p57^{KIP2} control muscle differentiation at the myogenin step. *Genes Dev.* 13, 213–224.
- Zhao, C., Zhou, Y., Liu, L., et al. (2018). Lipid accumulation in multi-walled carbon nanotube-exposed HepG2 cells: possible role of lipophagy pathway. *Food Chem. Toxicol.* 121, 65–71.
- Zhu, X., Xiong, T., Liu, P., et al. (2018). Quercetin ameliorates HFD-induced NAFLD by promoting hepatic VLDL assembly and lipophagy via the IRE1 α /XBP1s pathway. *Food Chem. Toxicol.* 114, 52–60.